

JOINT INSTITUTE FOR NUCLEAR RESEARCH  
Veksler and Baldin laboratory of High Energy Physics

**FINAL REPORT ON THE INTEREST PROGRAMME**

Study of bulk properties of the medium produced  
in heavy ion collisions at MPD

**Supervisor:**

Dr Alexey Aparin

**Student:**

Anil Sharma

UGC-DAE CSR Kolkata Center  
(University of Calcutta)

**Participation Period:**

February-April, Wave 8

Dubna, Russia - 2023

## DECLARATION

I, **Anil Sharma**, declare that the work presented in the project report titled "**Study of bulk properties of the medium produced in heavy ion collisions at MPD**" is my original work from **February to April 2023** and has not been submitted elsewhere for academic credit or publication. It has been carried out by me under the guidance of **Dr Alexey Aparin**, at Joint Institute for Nuclear Research, Veksler and Baldin laboratory of High Energy Physics.

I assert that all information and sources used in this project are accurately cited in the reference section, and I have given credit to all authors and contributors as appropriate.

I declare that I have adhered to ethical guidelines while conducting this research project, and all participants provided informed consent before their involvement. I also declare that I have not plagiarized any content or data during the research process and have taken all necessary measures to ensure that this work is original and follows ethical standards.

I acknowledge and understand that any violation of these ethical guidelines could result in severe consequences, including academic penalties, legal action, and loss of professional reputation.



Dr Alexey Aparin

(Anil Sharma)

Joint Institute for Nuclear Research,  
Dubna, Russia

# Acknowledgements

In completing this project report there is support, guidance and enhancement of many people without those it is not possible to prepare this report. I would like to express my sincere gratitude and appreciation to the following people and organizations who have contributed to the success of my research project titled:

- First and foremost, I would like to thank my project supervisor **Dr Alexey Aparin** for providing guidance and support throughout the entire project. Their insights, feedback, and expertise have been invaluable, and I am grateful for their mentorship.
- I would like to acknowledge the participants of this project who generously gave their time and effort to provide data and insights. Their contributions were essential to the success of this project, and I am indebted to them for their cooperation.
- I would also like to express my gratitude to my friends who provided support, feedback, and encouragement throughout the research process. Their insights and ideas helped to shape this project and contributed to its overall success.
- Finally, I would like to acknowledge the academic institutions or departments that have provided resources, facilities, and infrastructure for this research project. Their support has been crucial in enabling the research process and ensuring its success.

I acknowledge that without the support of these individuals and organizations, this research project would not have been possible.

# Abstract

Analysis of identified particle production can be a useful tool to measure the bulk properties of the medium produced in heavy ion collisions at high energies. As a part of preparations for the start of the NICA collider with the MPD experiment designed for the studies of hot and dense nuclear matter, we analyze MC model data on identified particle production at a set of different collision energies. So, we present the measurement of bulk properties of the matter produced in Bi+Bi collisions at  $\sqrt{s_{NN}} = 9.2 \text{ GeV}$  using the identified hadrons ( $\pi^\pm$ ),  $K^\pm$ , *proton*( $p$ ) from the MPD experiment at the Nuclotron-based Ion Collider fAcility (NICA). We are generating the data of Bi+Bi collisions by the statistical Monte Carlo generator model named Ultrarelativistic Quantum Molecular Dynamics (UrQMD). We analysis this data using the MpdRoot framework.

Results of Reconstructed tracks, Midrapidity( $y$ ), transverse momenta( $p_T$ ), Event selection region, distributions of the vertex Z, and distribution of the distance of closest approach(DCA) of the tracks are presented. These results constitute the relations of Energy loss( $dE/dx$ ) and total momentum( $P$ ) curve to identify the particles, also rapidity and transverse momentum( $p_T$ ) plot to figure out the cuts for further analysis.

# Contents

<b>Candidate's Declaration</b>	<b>1</b>
<b>Acknowledgements</b>	<b>2</b>
<b>Abstract</b>	<b>3</b>
<b>List of Figures</b>	<b>5</b>
<b>1 Introduction</b>	<b>7</b>
<b>2 NICA complex and Multi-Purpose detector</b>	<b>8</b>
2.1 NICA complex . . . . .	8
2.2 Multi-Purpose Detector . . . . .	10
<b>3 Project goals</b>	<b>11</b>
<b>4 Data Analysis for Experiment</b>	<b>12</b>
4.1 Event Selection . . . . .	12
4.2 Track Selection . . . . .	13
4.3 Particle Identification . . . . .	16
4.4 TPC Acceptance . . . . .	16
<b>5 Discussion and Future scope of work</b>	<b>17</b>
<b>References</b>	<b>19</b>

## List of Figures

1	The NICA accelerator complex at JINR. . . . .	7
2	QCD Phase diagram with chemical potential( $\mu_B$ ) on the horizontal axis and Temperature(T in MeV) on the vertical axis. It shows the regions, where various experiment facilities are working at the present time. . . . .	9
3	A general view of the MPD detector with end doors retracted for access to the inner detector components. . . . .	10
4	The event vertex x and y of the reconstructed event in Bi+Bi collisions at $\sqrt{s_{NN}} = 9.2\text{GeV}$ . . . . .	12
5	The event vertex x and y of the reconstructed event in Bi+Bi collisions at $\sqrt{s_{NN}} = 9.2\text{GeV}$ with the cuts at $ y  < 0.1$ . . . . .	12
6	The distributions of the primary vertex z in Bi+Bi collisions at $\sqrt{s_{NN}} = 9.2\text{GeV}$ . . . . .	13
7	The distributions of the primary vertex z in Bi+Bi collisions at $\sqrt{s_{NN}} = 9.2\text{GeV}$ with cuts at $ y  < 0.1$ . . . . .	13
8	Plot of the Number of hits which is showing the minimum( 10) and maximum( 53) number of hits for Bi+Bi collisions at $\sqrt{s_{NN}} = 9.2\text{GeV}$ . . . . .	13
9	Plot of the Number of hits which is showing the minimum( 10) and maximum( 53) number of hits for Bi+Bi collisions at $\sqrt{s_{NN}} = 9.2\text{GeV}$ with cuts at $ y  < 0.1$ . . . . .	13
10	The distributions of the DCA in Bi+Bi collisions at $\sqrt{s_{NN}} = 9.2\text{GeV}$ in 100 bins. . . . .	14
11	The distributions of the DCA in Bi+Bi collisions at $\sqrt{s_{NN}} = 9.2\text{GeV}$ with cuts at $ y  < 0.1$ in 100 bins. . . . .	14
12	This is the plot of the Number of hits to build the track with the transverse momentum( $p_T$ ) for Bi+Bi collisions at $\sqrt{s_{NN}} = 9.2\text{GeV}$ . . . . .	14
13	This is the plot of the Number of hits to build the track with the transverse momentum( $p_T$ ) for Bi+Bi collisions at $\sqrt{s_{NN}} = 9.2\text{GeV}$ with cuts at $ y  < 0.1$ . . . . .	14
14	Plot of the pseudorapidity in Bi+Bi collisions at $\sqrt{s_{NN}} = 9.2\text{GeV}$ in 200 bins. . . . .	15
15	Plot of the pseudorapidity in Bi+Bi collisions at $\sqrt{s_{NN}} = 9.2\text{GeV}$ with cuts at $ y  < 0.1$ in 200 bins. . . . .	15
16	Plot of the rapidity in Bi+Bi collisions at $\sqrt{s_{NN}} = 9.2\text{GeV}$ in 50 bins. . . . .	15
17	Plot of the rapidity in Bi+Bi collisions at $\sqrt{s_{NN}} = 9.2\text{GeV}$ with cuts at $ y  < 0.1$ in 50 bins. . . . .	15
18	The dE/dx of charged tracks with the total momentum(P) for Bi+Bi collisions at $\sqrt{s_{NN}} = 9.2\text{GeV}$ . . . . .	16
19	The dE/dx of charged tracks with the total momentum(P) for Bi+Bi collisions at $\sqrt{s_{NN}} = 9.2\text{GeV}$ with cuts at $ y  < 0.1$ . . . . .	16

20	Plot of rapidity( $y$ ) vs transverse momentum( $p_T$ ) for TPC acceptance for Bi+Bi collisions at $\sqrt{s_{NN}} = 9.2\text{GeV}$ . . . . .	17
21	Plot of rapidity( $y$ ) vs transverse momentum( $p_T$ ) for TPC acceptance for Bi+Bi collisions at $\sqrt{s_{NN}} = 9.2\text{GeV}$ with cuts at $ y  < 0.1$ . . . . .	17
22	Plot of transverse momentum( $p_T$ ) spectra for Bi+Bi collisions at $\sqrt{s_{NN}} = 9.2\text{GeV}$ in 100 bins. . . . .	18
23	Plot of transverse momentum( $p_T$ ) spectra for Bi+Bi collisions at $\sqrt{s_{NN}} = 9.2\text{GeV}$ with cuts at $ y  < 0.1$ in 100 bins. . . . .	18
24	Plot of total momentum( $P_{tot}$ ) for Bi+Bi collisions at $\sqrt{s_{NN}} = 9.2\text{GeV}$ in 100 bins. . . . .	18
25	Plot of total momentum( $P_{tot}$ ) for Bi+Bi collisions at $\sqrt{s_{NN}} = 9.2\text{GeV}$ with cuts at $ y  < 0.1$ in 100 bins. . . . .	18

# 1 Introduction

In modern physics, a very challenging task is to investigate hot and dense baryonic matter. This investigation can provide us with very useful information about the in-medium properties of hadrons and nuclear matter equation of state and also can give us an idea of the evolution of the early universe and formation of the neutron stars and other astrophysical objects as well. So to carry out this research, a vast research program of basic sciences is going on over the last two decades. The main centers which are equipped with high energy ion accelerators are GSI Helmholtz Centre for Heavy Ion Research(Germany), The Super Proton Synchrotron - CERN(Geneva), BNL-Relativistic High Ion Collider(USA), and JINR - SPh - Nuclotron (Russia).

From the recent observations for the creation of a new kind of Quantum Chromodynamic (QCD) matter and the strongly interacting quark-gluon plasma(SQGP), the theoretical comprehension of these data is far from being complete, which gives us the drive for different laboratories to undertake new efforts in the domain of heavy-ion physics. JINR scientific program is dedicated to the study of hot and dense baryonic matter. To achieve this goal, a new JINR accelerated complex- named the Nuclotron-based Ion Collider Facility (NICA) [1] has been constructed to provide the heavy ions collisions over a wide range of atomic masses. The NICA collider complex is shown below in figure [1].

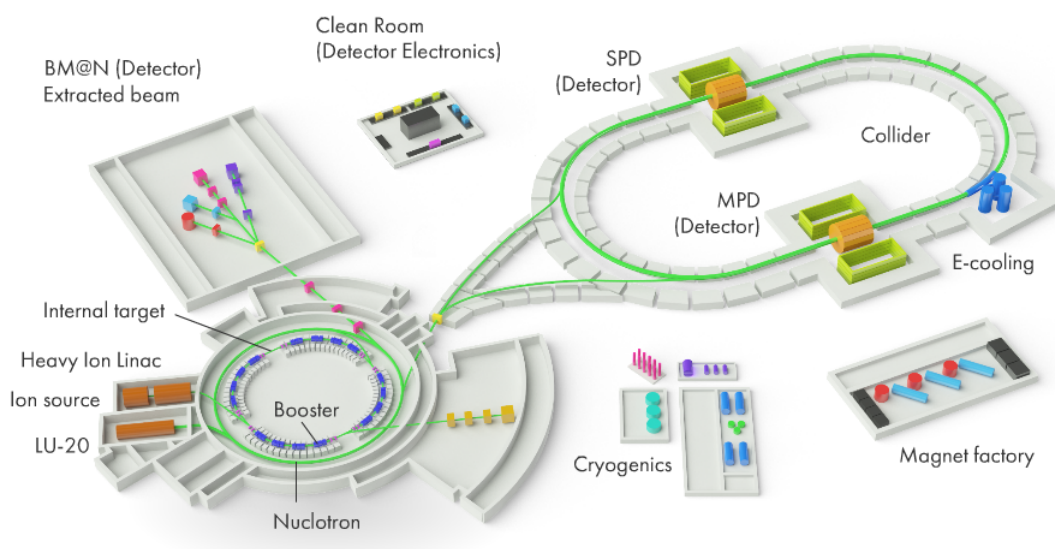


Figure 1: The NICA accelerator complex at JINR.

## 2 NICA complex and Multi-Purpose detector

This section presents the NICA complex and Multi-Purpose Detector concepts for the international heavy-ion research facility proposed by the JINR to investigate the basic QCD structure of matter [2]. This facility takes into account the broadened scope of the physics of strong interaction and problems related to the fundamental many-body systems and provides particle beams.

### 2.1 NICA complex

The international mega-science project "NICA complex" is aimed at the study of the properties of nuclear matter in the region of the maximum baryon density. Such type of matter can only exist in the early stages of the evolution of our universe and in the interiors of neutron stars. From the past research done by many scientists about lattice QCD calculations, we can predict both the deconfinement phase transition and chiral symmetry restoration to happen at high energy densities and there is strong experimental evidence that the deconfined phase of nuclear matter or QGP can be created in ultra high energy nuclear collisions [3].

Also, the Experimental data on hadron production properties at SPS(Cern) suggest that this transition occurs within the NICA energy range. In addition, this range is sufficiently large to encompass both, collisions in which the plasma phase is well developed and collisions in which the matter remains purely hadronic throughout. After all of this, the phase diagram of strongly interacting matter contains a critical point and its experimental identification forms a focal point for this research field. Check below the QCD phase diagram in Figure [2].

There are some physics tasks of the NICA heavy-ion program to be studied for different ion by scanning in energy range from 3 to 11 GeV;

- Event-by-event fluctuation in hadron productions (multiplicity, transverse momentum( $p_T$ ) etc.
- Femtoscopic correlation.
- Directed and elliptic flows for various hadrons.
- Multi-strange hyperon production (including hypernuclei): yield and spectra (the probes of nuclear media phases).
- Photon and electron probes.
- Charge asymmetry.

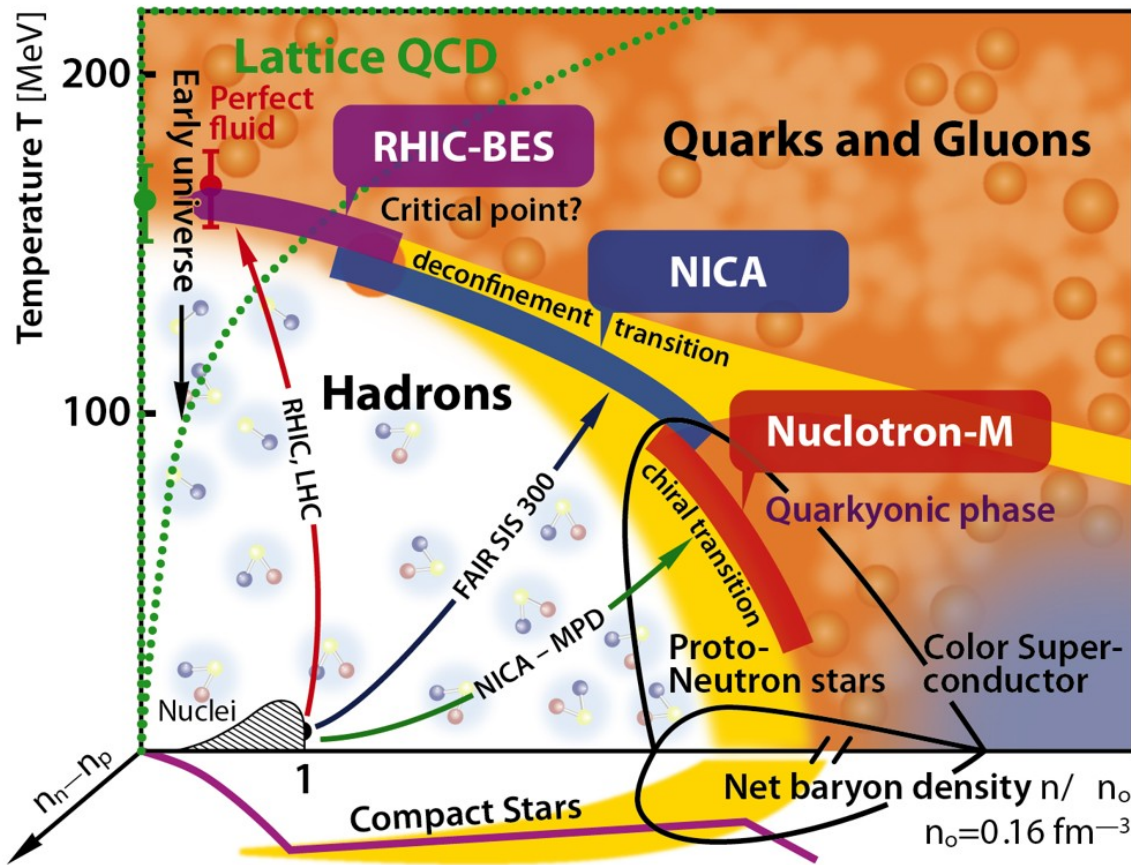


Figure 2: QCD Phase diagram with chemical potential( $\mu_B$ ) on the horizontal axis and Temperature( $T$  in MeV) on the vertical axis. It shows the regions, where various experiment facilities are working at the present time.

The study of strange particles [4] is of interest because we know from the theoretical predictions that the strangeness enhancement in heavy-ion-induced interactions might be a key to the deconfinement phase transitions. Moreover, nuclear objects with strangeness- hypernuclei can be formed inside the fireball, and since the energy range of the NICA covers the region of the maximal baryon density of the production rates of nuclear clusters with strangeness are predicted to be enhanced considerably.

Thus, the outcome of the NICA program, in particular, new experimental data on (anti)hyperon and hypernuclei production which will be taken with the MPD detector will provide valuable insight into the reaction dynamics and properties of the QCD matter [5].

## 2.2 Multi-Purpose Detector

The main physics experiment at the NICA complex is the Multi-Purpose Detector (MPD) [6] which is operating at the collider. This experimental program includes simultaneous measurements of observables that are presumably sensitive to high nuclear density effects and phase transitions. The software framework for the MPD experiment is MpdRoot, which is based on FairRoot and provides a powerful tool for detector performance studies, development of algorithms for reconstruction, and physics analysis of the experimental data.

For this, we use an extended set of event generators for heavy ion collisions like Ultrarelativistic Quantum Molecular Dynamics (UrQMD), Quark Gluon String Model (QGSM, LAQGSM) etc. The MPD apparatus is shown schematically in Figure [3].

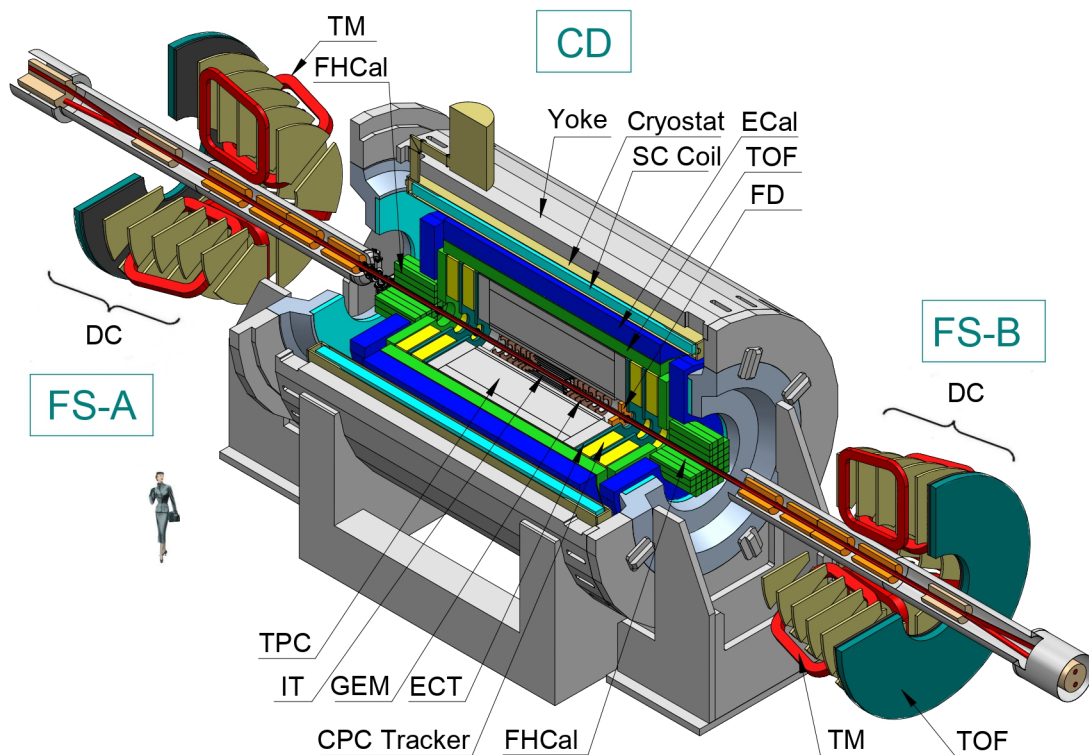


Figure 3: A general view of the MPD detector with end doors retracted for access to the inner detector components.

The MPD detector has been designed as a  $4\pi$  spectrometer capable of detecting particle's hadrons, electrons, and photons in heavy-ion collisions at high luminosity. To reach this goal, the detector will comprise a precise 3D tracking system and a high-performance particle identification (PID) system based on

time of flight (TOF) measurement and calorimetry. The basic design parameters have been determined taking into account the physics measurements to be performed and several technical constraints guided by a trade-off of efficient tracking and PID against a reasonable material budget.

In MPD experiment, the beamline is surrounded by the large gaseous Time Projection Chamber (TPC) which is enclosed by the Time-of-Flight (TOF) barrel. The Electromagnetic Calorimeter (EMCal) is placed between the TOF and the MPD magnet. It will be used for detection of electromagnetic showers, and will play the main role in photon and electron measurements. The First Forward Detector (FFD) is located in the forward direction within the TPC barrel. It plays the role of a wakeup trigger. The Forward Hadronic Calorimeter (FHCAL) is located near the Magnet endcaps. It determines the collision centrality and the orientation of the reaction plane for collective flow studies. The silicon-based Inner Tracker System (ITS) will be installed close to the interaction point in the second stage of the MPD construction. It will greatly enhance tracking and secondary vertex reconstruction capabilities. The miniBeBe detector placed between the beam pipe and the TPC, close to the beam, and designed to aid in triggering and start time determination for the TOF. The MPD Cosmic Ray Detector (MCORD), installed on the outside of the MPD Magnet Yoke, will measure muons, also from the cosmic showers.

We are expecting that the MPD will produce event-by-event information on charged particle tracks coming from the primary interaction vertices, together with identification of those particles, and information on the collision centrality. The MPD identification power obtained for charged hadrons with combined mass-squared ( $m^2$ ) from TOF and energy loss per distance ( $dE/dx$ ) from TPC [7].

### 3 Project goals

The project comes under the preparations for the NICA MPD experiment, and has the main goal of using MPD software, simulation, and Monte Carlo data to recreate experimental conditions for the Bi+Bi collisions of the MPD experiment at  $\sqrt{s_{NN}} = 9.2$  GeV. We are going to obtain the results on transverse momentum ( $p_T$ ) spectra, radial position of the event vertex, track selection for TPC, Particle identification from the experimental data, the distance of closest approach (DCA) between each track and the event vertex and then the cuts using the rapidity and total momentum analysis.

## 4 Data Analysis for Experiment

For the analysis, we are using the simulated data in this project work which was obtained by the Monte Carlo method using the generators UrQMD [8] and undergo the entire chain of reconstruction on the condition of real Bi+Bi collisions of the MPD experiment with the center-of-mass energy of  $\sqrt{s_{NN}} = 9.2\text{GeV}$ .

### 4.1 Event Selection

The criteria for minimum bias-triggered event selection begin with the identification of a primary vertex that is the common point of origin of tracks in an event which is measured by the TPC. Figure [4](without cuts) shows the x and y positions of the primary vertex in 7.2 GeV Bi+Bi collisions. In order to reject the background events, which involve interactions with the beam pipe of radius 6 cm, the event vertex radius is required to be within 4 cm of the center of the MPD detector. The ring of a black dense area of data points in Figure [4](without cuts) and [5](with cuts) corresponds to collisions between the beam nuclei and the beam pipe. This type of background is more significant and useful in low-energy data.

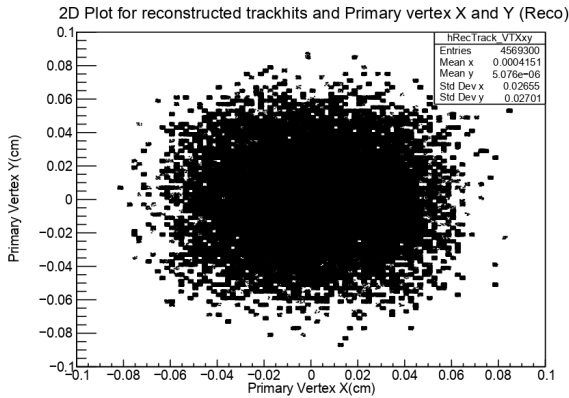


Figure 4: The event vertex x and y of the reconstructed event in Bi+Bi collisions at  $\sqrt{s_{NN}} = 9.2\text{GeV}$ .

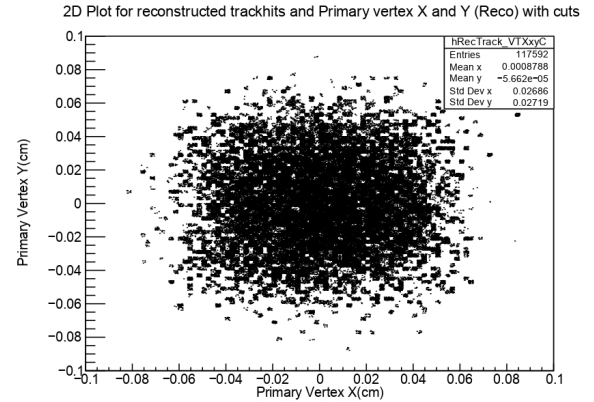


Figure 5: The event vertex x and y of the reconstructed event in Bi+Bi collisions at  $\sqrt{s_{NN}} = 9.2\text{GeV}$  with the cuts at  $|y| < 0.1$ .

The distributions of the primary vertex position along the longitudinal (beam) direction ( $V_z$ ) are shown in Figure [6](without cuts) and [7](with cuts) for 9.2 GeV Bi+Bi collisions. The wide z-vertex distribution at lower energies is due to the fact that the beams are more difficult to focus at lower energies. Only those events which have a  $V_z$  within 50 cm were selected for the analysis. These values are chosen to achieve uniform detector performance and sufficient statistical significance of the measured observable. In Figure [6](without

cuts), we can see that the total number of events used for analysis is around  $10^4$  to  $10^5$  and entries are 4569300 at the energy of 9.2 GeV.

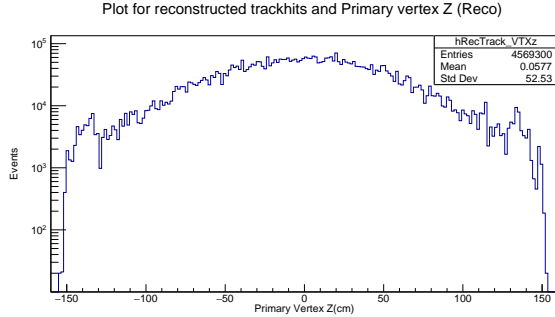


Figure 6: The distributions of the primary vertex z in Bi+Bi collisions at  $\sqrt{s_{NN}} = 9.2\text{GeV}$ .

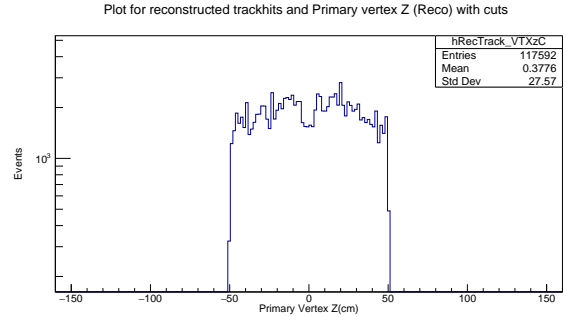


Figure 7: The distributions of the primary vertex z in Bi+Bi collisions at  $\sqrt{s_{NN}} = 9.2\text{GeV}$  with cuts at  $|y| < 0.1$ .

## 4.2 Track Selection

Track selection criteria are necessary for analyses. The tracks that extrapolate to TOF active cells have already been selected for at least two criteria: The number of hits [9] and momentum. In Figure [8](without cuts) and [9](with cuts), we can see that tracks must have at least 10 points used in track fitting out of the maximum of 53 hits possible in the TPC. To prevent multiple counting of split tracks, at least 19% of the total possible fit points are required.

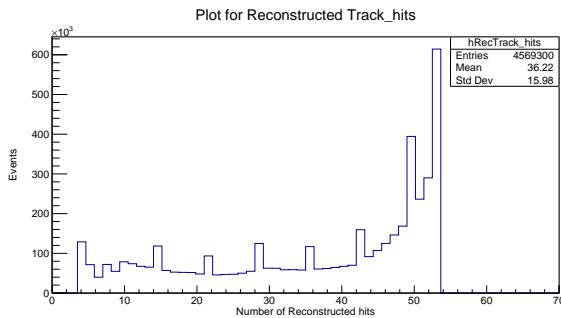


Figure 8: Plot of the Number of hits which is showing the minimum ( 10) and maximum( 53) number of hits for Bi+Bi collisions at  $\sqrt{s_{NN}} = 9.2\text{GeV}$ .

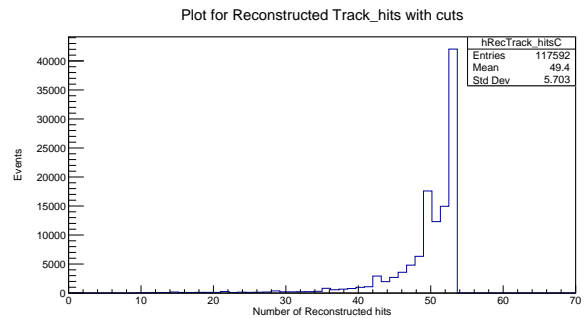


Figure 9: Plot of the Number of hits which is showing the minimum( 10) and maximum( 53) number of hits for Bi+Bi collisions at  $\sqrt{s_{NN}} = 9.2\text{GeV}$  with cuts at  $|y| < 0.1$ .

In order to suppress the admixture of tracks from secondary vertices, a requirement of less than 3 cm is placed on the distance of the closest approach (DCA) between each track and the event vertex. We can clearly see this in our DCA plot, in Figure [10](without cuts) and [11](with cuts) as well.

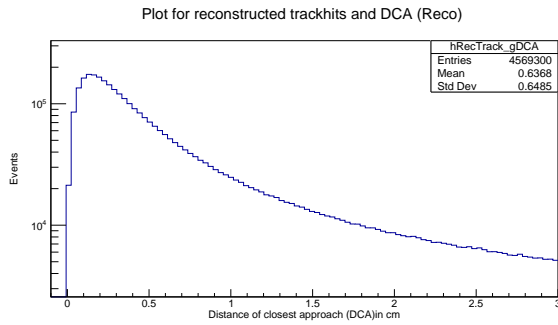


Figure 10: The distributions of the DCA in Bi+Bi collisions at  $\sqrt{s_{NN}} = 9.2\text{GeV}$  in 100 bins.

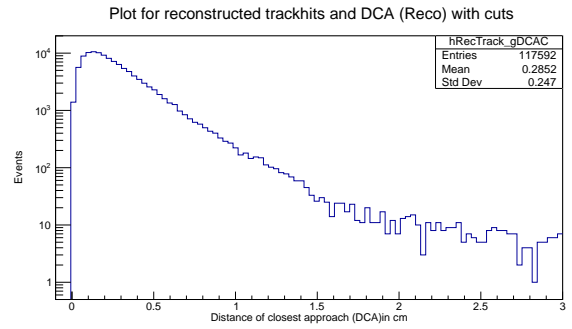


Figure 11: The distributions of the DCA in Bi+Bi collisions at  $\sqrt{s_{NN}} = 9.2\text{GeV}$  with cuts at  $|y| < 0.1$  in 100 bins.

In Figure [12](without cuts) and [13](with cuts), the total momentum of charge particles appears at 0.1 GeV/c because particles with lower momenta would spiral in the magnetic field and will not reach the TOF elements.

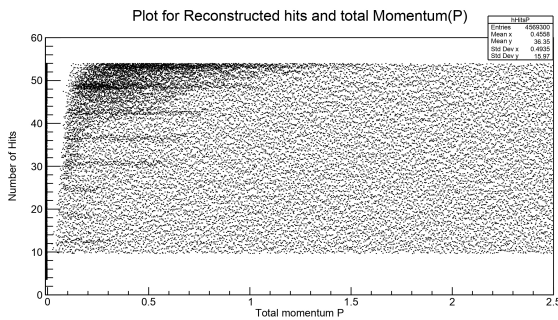


Figure 12: This is the plot of the Number of hits to build the track with the transverse momentum( $p_T$ ) for Bi+Bi collisions at  $\sqrt{s_{NN}} = 9.2\text{GeV}$ .

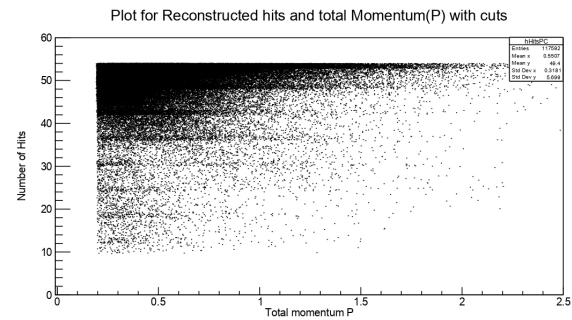


Figure 13: This is the plot of the Number of hits to build the track with the transverse momentum( $p_T$ ) for Bi+Bi collisions at  $\sqrt{s_{NN}} = 9.2\text{GeV}$  with cuts at  $|y| < 0.1$ .

Now let's discuss Rapidity and Pseudorapidity [10]: so basically, Pseudorapidity is a quantity used in high-energy physics to describe the angle of a particle relative to the beam axis in a particle collision experiment. It is defined as:

$$\eta = -\log\left[\tan\left(\frac{\theta}{2}\right)\right] \quad (4.2.1)$$

where  $\theta$  is the angle between the direction of the particle and the beam axis.

Pseudorapidity is a useful quantity because it is related to the rapidity of a particle, which is a quantity that is invariant under Lorentz transformations in

the longitudinal direction. Rapidity is defined as:

$$y = \frac{1}{2} \log \left[ \frac{P_{tot} + p_z}{P_{tot} - p_z} \right] \quad (4.2.2)$$

where  $P_{tot}$  is the total momentum of the particle and  $p_z$  is its momentum along the beam axis.

As we know already know Pseudorapidity and Rapidity describe the distributions of particles, which we can see in Figure [14](without cuts), [15](with cuts), and Figure [16](without cuts), [17](with cuts).

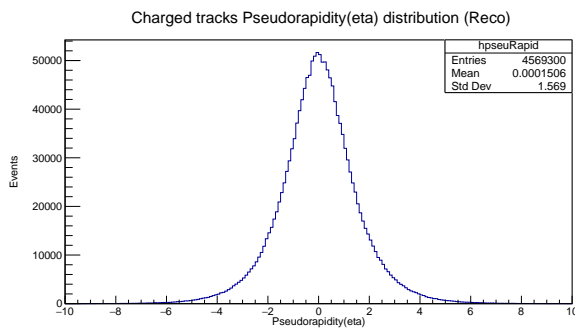


Figure 14: Plot of the pseudorapidity in Bi+Bi collisions at  $\sqrt{s_{NN}} = 9.2\text{GeV}$  in 200 bins.

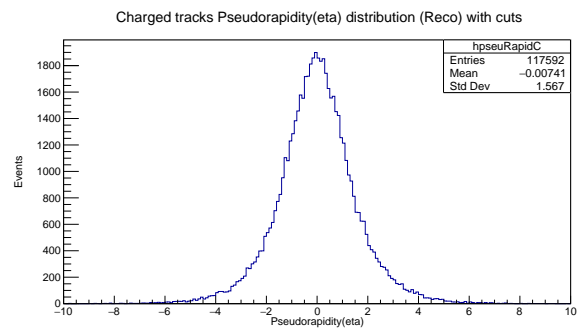


Figure 15: Plot of the pseudorapidity in Bi+Bi collisions at  $\sqrt{s_{NN}} = 9.2\text{GeV}$  with cuts at  $|y| < 0.1$  in 200 bins.

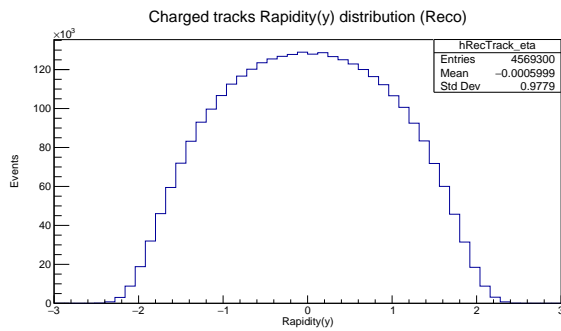


Figure 16: Plot of the rapidity in Bi+Bi collisions at  $\sqrt{s_{NN}} = 9.2\text{GeV}$  in 50 bins.

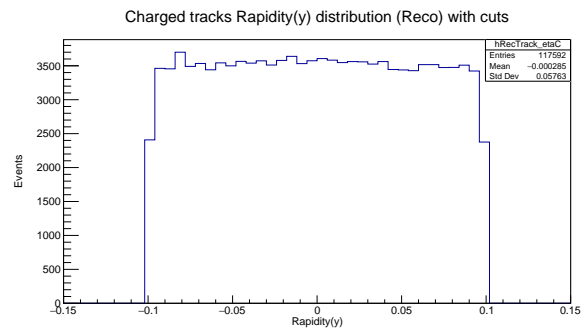


Figure 17: Plot of the rapidity in Bi+Bi collisions at  $\sqrt{s_{NN}} = 9.2\text{GeV}$  with cuts at  $|y| < 0.1$  in 50 bins.

So we need to select a constant region to study and for analysis. That's why, we are doing the cuts for rapidity in the  $|y| < 0.1$  region, see the Figure [17] for the region of the cuts. And we will be going to keep the same track cuts for all energies.

### 4.3 Particle Identification

Particle identification is accomplished in the TPC by measuring the energy loss ( $dE/dx$ ). Figure [18](without cuts) and [19](with cuts) shows the energy loss  $dE/dx$  of measured charged particles plotted with the total momentum( $P$ ) of the particles. At the low momentum, it can be seen that the TPC can identify the pions ( $\pi^\pm$ ) (in -0.2 to -0.1 and 0.1 to 0.2 region), kaons ( $k^\pm$ ) (in -0.5 to -0.2 and 0.2 to 0.5 region), protons ( $p$ ) (in 0.5 to 1 region), and antiprotons ( $\bar{p}$ ) (in -1 to -0.5 region). If we try to fit this plot for these regions, we will get similar results to the Bischel expectation values. At low  $p_T$ , the peaks of pion, kaon, and proton distributions are well separated. However, at higher  $p_T$  these distributions start to overlap.

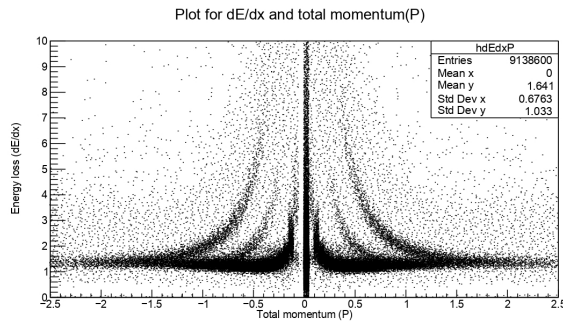


Figure 18: The  $dE/dx$  of charged tracks with the total momentum( $P$ ) for Bi+Bi collisions at  $\sqrt{s_{NN}} = 9.2\text{GeV}$ .

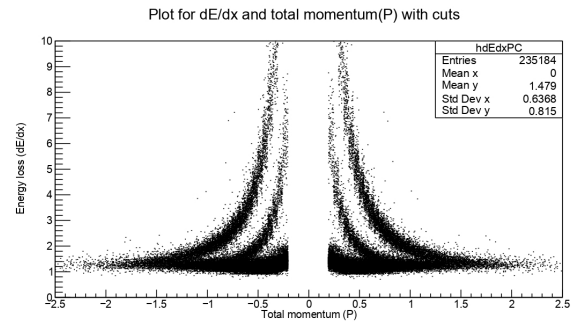


Figure 19: The  $dE/dx$  of charged tracks with the total momentum( $P$ ) for Bi+Bi collisions at  $\sqrt{s_{NN}} = 9.2\text{GeV}$  with cuts at  $|y| < 0.1$ .

### 4.4 TPC Acceptance

Finally, for TPC acceptance, the selection criteria and needed cuts for all energies are:

- Number of hits/points,  $N_{hits} > 10$ ,
- Only charged particles taken in account,
- Rapidity,  $|y| < 0.1$ ,
- Primary vertex  $Z < 50$  cm,
- Total momenta of the particles( $P_{tot}$ )  $> 0.1$  GeV/c,
- Transverse momenta for the particles( $p_T$ )  $> 0.2$  GeV/c,
- Distance of closest approach(DCA)  $< 3$  cm,

- Bi+Bi collisions for the center of mass energy  $\sqrt{s_{NN}} = 9.2\text{GeV}$  using the generator UrQMD.

You can see the Figure [20](without cuts) and [21](with cuts) for the transverse momenta( $p_T$ ) with rapidity( $y$ ) and from this, we can figure out the most collisions of particles in our detector.

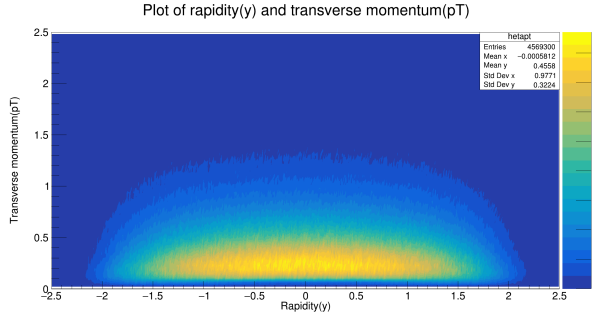


Figure 20: Plot of rapidity( $y$ ) vs transverse momentum( $p_T$ ) for TPC acceptance for Bi+Bi collisions at  $\sqrt{s_{NN}} = 9.2\text{GeV}$ .

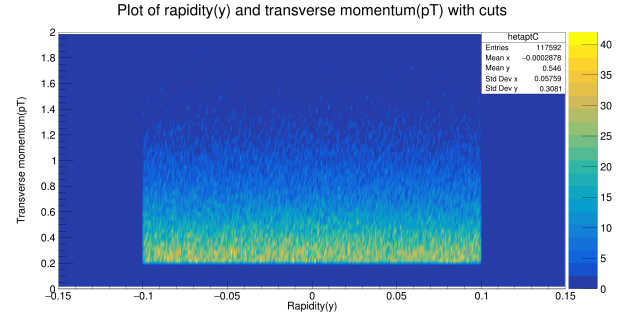


Figure 21: Plot of rapidity( $y$ ) vs transverse momentum( $p_T$ ) for TPC acceptance for Bi+Bi collisions at  $\sqrt{s_{NN}} = 9.2\text{GeV}$  with cuts at  $|y| < 0.1$ .

## 5 Discussion and Future scope of work

In this project, Monte Carlo data of Bi+Bi heavy ion collisions in the center-of-mass energy range is analyzed  $\sqrt{s_{NN}} = 9.2\text{GeV}$ . Also, several other studies have been performed to improve the quality of particle identification and made some cuts for better results or analysis like DCA cuts, rapidity cuts, the minimum number of hits, etc. From these cuts and analysis, we got the spectra for transverse momenta ( $p_T$ ), in Figure [22] (without cuts), [23] (with cuts), and total momenta ( $P_{tot}$ ) in Figure [24] (without cuts), [25] (with cuts). For further analysis, it is necessary to analyze more statistical data using different Monte Carlo models for different values of the collision energy of the center of mass etc.

For future scope, we are aiming to contribute to the studies of bulk properties of this system for an incoming run of the MPD/NICA experiment. For preliminary results of the first runs on the NICA complex facilities with Bi+Bi heavy ion collisions at low energies, previously done studies of first physics are necessary. This work can lead us to the chemical and kinetic freeze-out dynamics at these energies. That's why, I am looking forward to visiting the JINR facility for further work. There, we can also work on centrality dependence for particle production, particle yields, particle ratio, the energy dependence of particle production, and freeze-out parameters. In the end, we can find out the

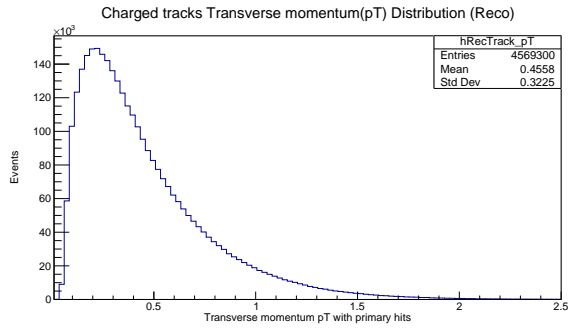


Figure 22: Plot of transverse momentum( $p_T$ ) spectra for Bi+Bi collisions at  $\sqrt{s_{NN}} = 9.2\text{GeV}$  in 100 bins.

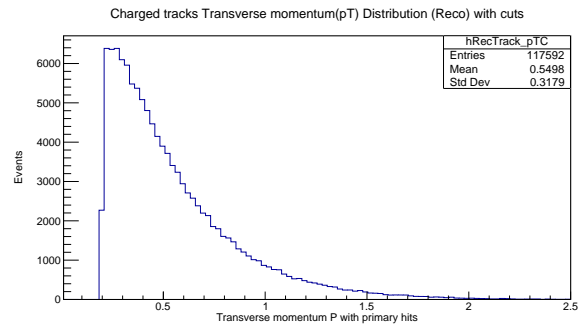


Figure 23: Plot of transverse momentum( $p_T$ ) spectra for Bi+Bi collisions at  $\sqrt{s_{NN}} = 9.2\text{GeV}$  with cuts at  $|y| < 0.1$  in 100 bins.

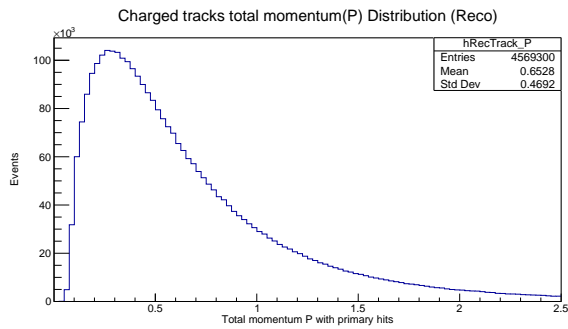


Figure 24: Plot of total momentum( $P_{tot}$ ) for Bi+Bi collisions at  $\sqrt{s_{NN}} = 9.2\text{GeV}$  in 100 bins.

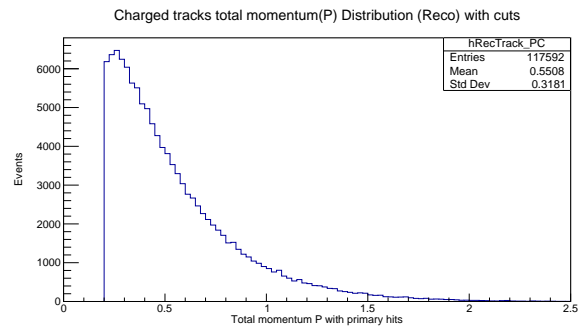


Figure 25: Plot of total momentum( $P_{tot}$ ) for Bi+Bi collisions at  $\sqrt{s_{NN}} = 9.2\text{GeV}$  with cuts at  $|y| < 0.1$  in 100 bins.

relation of temperature( $T$ ) and chemical potential( $\mu_B$ ) for the phase diagram to search for the QCD critical point.

I am attaching my GitHub link [11] for this analysis so you can do it by yourself. Also, you can give suggestions for improvement in this code if you think it's necessary.

## References

- [1] Website for nica complex facility, <https://nica.jinr.ru/>.
- [2] I. Arsene and I.G. Bearden et. al. Quarkgluon plasma and color glass condensate at rhic, the perspective from the brahms experiment. *Nuclear Physics A*, 757(1):1–27, 2005. First Three Years of Operation of RHIC.
- [3] M. S. Abdallah et al. Pion, kaon, and (anti)proton production in U+U collisions at  $\sqrt{s_{NN}}=193$  GeV measured with the STAR detector. *Phys. Rev. C*, 107(2):024901, 2023.
- [4] J. Adam and et. al. Adamczyk. Strange hadron production in Au + Au collisions at  $\sqrt{s_{NN}} = 7.7, 11.5, 19.6, 27, \text{ and } 39$  gev. *Phys. Rev. C*, 102:034909, Sep 2020.
- [5] L. Adamczyk and et. al. Adkins. Bulk properties of the medium produced in relativistic heavy-ion collisions from the beam energy scan program. *Phys. Rev. C*, 96:044904, Oct 2017.
- [6] Website for mpd detector facility, <http://mpd.jinr.ru/>.
- [7] L Yordanova and V Vasendina. Mpd detector at nica. *Journal of Physics: Conference Series*, 503(1):012041, apr 2014.
- [8] Urqmd official website, <https://urqmd.org/>.
- [9] R. Debbe. Time of flight track matching efficiency in star experiment, <https://drupal.star.bnl.gov/STAR/files/userfiles/2729/file/T0FmatchingNote.pdf>.
- [10] Dr.ssa Barbara Guerzoni. Identified primary hadron spectra with the tof detector of the alice experiment at lhc, <https://cds.cern.ch/record/1495621/files/tesiGuerzoniDottorato.pdf>.
- [11] Github link of the code, which i wrote for this analysis, [https://github.com/Hachiman512/Cutting\\_in\\_MPD.git](https://github.com/Hachiman512/Cutting_in_MPD.git).